

# Combined Motion Design and Control of Multi-Stage Flexible Telescopic Boom Model

Wen-zheng DU, Peng WU, Xia WU, Bao-zhu MA

Xi'an High Institution, Xi'an Shaanxi 710025

**Key words :** Flexible multi-stage telescopic ; System Model; Combined motion; simulation analysis; experiment

**Abstract:** To solve the problem of flexible multi-stage telescopic boom automatic reprint, according to ADAMS flexible body modeling theory, electro-hydraulic proportional position control theory and co-simulation modeling interface technology to establish flexible multi-stage telescopic system model based on virtual prototype. On the basis of model, integrated telescopic boom crane movement characteristics, designed and calculated the movement of the three combined motions. Introduced PID control algorithm and achieving a combination of joint motion by virtual prototype simulation technology. Viewed the results of the end of telescopic boom trajectory and dynamics in the ADAMS processing unit. Verified by experiments and The results show that: the flexible multi-stage telescopic boom system model can achieve a combination of motion control and control is better. The research content provide some reference to improve the crane automatically reprint efficiency and reduce the number of physical prototype tests.

## 1 Introduction

With the number of telescopic boom increased, lightweight and flexible structure features more obvious, the speed of reprint, the contradiction between stability and safety become more and more prominent. Therefore, in order to study the security, accuracy and efficiency of the docking process and reduce the number of physical prototypes, a kinetic model which can accurately reflect the process of flexible telescopic arm transport is established<sup>[1]</sup>, Which reflects the motion characteristics of telescopic boom.

The combination of motion design in three typical conditions: the vertical plane linear motion, the horizontal plane linear motion and the spatial range linear motion. Three movements in the actual work on behalf of the lifting weight along the vertical line, along the horizontal line transfer of heavy objects, as well as some of the hinge points of mechanical equipment to achieve vertical lifting. The three motion modes are defined as

Multi-stage flexible telescopic boom system to achieve the combined movement, mainly through the calculation of hydraulic cylinder movement, control of telescopic movement, rotary motion and luffing movement, to complete the expected repose trajectory or combination of actions<sup>[2,3]</sup>. The PID control algorithm is introduced in the control system. After the optimization of the control parameters, the simulating experiments of the typical process of the telescopic boom are carried out according to the expected movement rule. The dynamic response of the multi-stage flexible telescopic boom is analyzed and compared with the experimental results. Accuracy and practicability of the whole system model of flexible telescopic boom.

## 2 Subject

Based on the actual dimensions of the multi-stage telescopic boom experimental platform, the parts of the basic arm, the primary arm, the secondary arm, the support cylinder, the telescopic cylinder and the support were established by using the SolidWorks. All the parts were assembled and analyzed by ANSYS. The flexible telescopic boom are introduced into ADAMS to establish a multi-stage flexible telescopic boom mechanical system model<sup>[4-6]</sup>. In the restraining way of the telescopic arm used contact mode<sup>[5,10]</sup>. The hydraulic system model and the control system model of the telescopic boom system were established by MATLAB/Simulink and the system simulation model was established by using co-simulation technology<sup>[7,9]</sup>. Figure1 is a multi-stage flexible telescopic boom simulation

3D MODEL

SIMULATION MODEL

The diagram illustrates a closed-loop control system. A sine wave input enters an adder block (+). The output of the adder goes through two integrators (In1 Out1 and In2). The output of the second integrator branches off to a scope labeled 'velocity'. Another branch from the same point goes through a gain block labeled '反馈系数' (Feedback Coefficient) with a value of 1, which then feeds back into the negative input of the adder block. The main signal path continues from the first integrator's output through a block labeled 'adams\_sub' (which contains a mechanical system model). This block has two outputs: one goes to a scope labeled 'displacement', and the other goes to a summing junction (+). The output of the summing junction is fed back into the positive input of the adder block. Finally, the output of the summing junction also passes through a scope labeled 'Scope'.

264

From(1),(2):

$$h - h_1 = \sqrt{(x_0 + \Delta x_2)^2 - x_0^2} = vt_2 \quad (3)$$

(2) Law of pitch movement:

$$\cos \alpha = \frac{a^2 + b^2 - c_1^2}{2ab}, \quad \cos \alpha' = \frac{b^2 + c_1^2 - a^2}{2bc_1} \quad (4)$$

$$\cos\left(\frac{\pi}{2} - \alpha'\right) = \frac{c_1^2 + d^2 - y_0^2}{2c_1 d} \quad (5)$$

$$\cos \theta = \frac{(x_0 + \Delta x_1)^2 + (x_0 + \Delta x_2)^2 - h^2}{2(x_0 + \Delta x_1)(x_0 + \Delta x_2)} \quad (6)$$

$$\cos(\alpha + \theta) = \frac{a^2 + b^2 - c_2^2}{2ab} \quad (7)$$

$$\cos \beta = \frac{b^2 + c_2^2 - a^2}{2bc_2} \quad (8)$$

$$\cos\left(\frac{\pi}{2} - \beta\right) = \frac{c_2^2 + d^2 - (y_0 + \Delta y)^2}{2dc_2} \quad (9)$$

$x_0$ : The length of the arm when the telescopic boom is lifted;  $\Delta x_1$  the length of the telescopic boom;  $\Delta x_2$  the length of the telescopic boom in the horizontal position;  $\alpha$  the pitch angle in the initial state of the telescopic boom;  $h_1$  The vertical distance from lifting to the horizontal position;  $y_0$  the original length of the pitching mechanism;  $\Delta y$  the length of the lifting mechanism to the target state;  $\theta$  the angle of the lifting weight of the telescopic boom;  $a$  the distance between the supporting point of the cylinder and the rear hinge point of the telescopic boom;  $b$  the telescopic arm pivot point to support the cylinder after the hinge point of the vertical distance;  $c_1$ ,  $c_2$ ,  $\beta$  and  $\alpha'$  facilitate the geometric relationship between the auxiliary line and auxiliary angle added;  $d$  support the fuel tank after the hinge point and the distance between the support device;

### 3.2 the horizontal plane linear motion

Horizontal plane linear motion using telescopic mechanism and the coordination of the slewing mechanism, reducing the weight of the movement of the transfer line, improve the efficiency of reprint, the experiment fast and accurate reprint. Horizontal plane linear motion diagram shown in Figure 4:

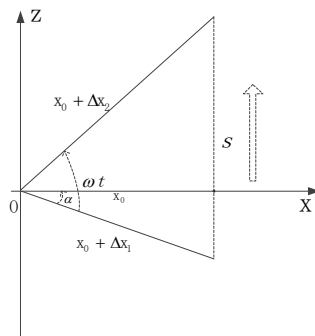


Fig.4 A horizontal plane diagram of linear motion

Suppose:  $l_0$ ,  $S$ ,  $\omega$ . According to the geometric model, the movement trajectory of the crane boom satisfies the following relation:

$$\cos \alpha = \frac{x_0}{(x_0 + \Delta x_1)}, l_0 = (x_0 + \Delta x_1) \quad (10)$$

$$\cos \omega t_1 = \frac{x_0}{(x_0 + \Delta x_1)} \quad (11)$$

$$\cos \omega(t-t_1) = \frac{x_0}{(x_0 + \Delta x_2)}, (t \geq t_1) \quad (12)$$

$$\tan[\omega(t-t_1)] = \frac{S - (x_0 + \Delta x_1) \sin \alpha}{x_0} \quad (13)$$

$$\cos(\omega t_2) = \frac{x_0}{x_0 + \Delta x_2}, t = t_1 + t_2 \quad (14)$$

$x_0$  The length of the arm when the telescopic arm is rotated to the state;  $\Delta x_2$  the extension of the arm length when the telescopic arm is rotated to the target state;  $\alpha$  the angle perpendicular to the locus of movement;  $t_1$ 、 $t_2$  the time taken to rotate to the two states.

### 3.3 the spatial range linear motion

Spatial range Linear motion is the lifting of the horizontal placement of the weight to the vertical state. The motion diagram is shown in Figure 5:

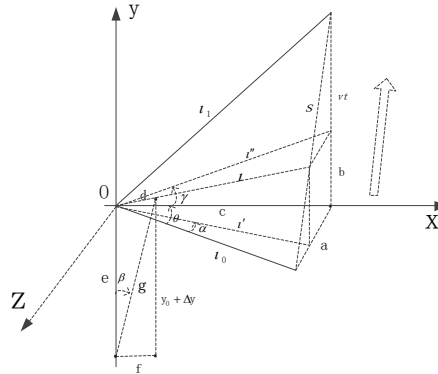


Fig.5 The spatial extent of linear motion sketch

Suppose:  $l_0$ ,  $b$ ,  $a$ ,  $\omega$ ,  $s = \sqrt{a^2 + b^2}$ , According to the geometric relationship presented by the geometric model, the state of the telescopic arm moves to an arbitrary position is analyzed. The geometric relationship between the trajectories of the crane boom is as follows:

#### 1) Solution of the length of the arm to move to any position

At any position, the projection of the telescopic arm in XOZ and XOY plane is  $l'$  and  $l''$ . the telescopic arm moves to arm length  $l$  when the rotation angle is  $\alpha$ , the pitch angle is  $\gamma$ , and:

$$c = \sqrt{l_0^2 - a^2}, \quad \theta = \arcsin \frac{a}{l_0} \quad (15)$$

$$l' = \frac{c}{\cos(\theta - \omega t)} \quad (16)$$

#### 2) Solving the law of arm length variation

$$l'' = \sqrt{c^2 + (vt)^2} \quad (17)$$

$$\cos \gamma = \frac{c}{l''} = \frac{c}{\sqrt{c^2 + (vt)^2}} \quad (18)$$

$$l = \frac{l'}{\cos \gamma} = \frac{\sqrt{c^2 + (vt)^2}}{\cos(\theta - \omega t)} \quad (19)$$

the law of arm length variation:

$$\Delta x = l - l_0 = \frac{\sqrt{c^2 + (vt)^2}}{\cos(\theta - \omega t)} - l_0 \quad (20)$$

$c$  the telescopic arm reaches the target position in the XOZ plane when the projection length;  $\theta$

telescopic arm in place for the target position to turn the angle.

### 3) Solving the law of pitch mechanism variation

To facilitate the solution of geometric relations, the introduction of auxiliary lines. From the geometric relations can get the following relationship:

$$\cos(\gamma + \frac{\pi}{2}) = \frac{d^2 + e^2 - g^2}{2de} \quad (21)$$

$$\cos \beta = \frac{e^2 + g^2 - d^2}{2eg} \quad (22)$$

$$\cos(\frac{\pi}{2} - \beta) = \frac{g^2 + f^2 - (y_0 + \Delta y)^2}{2gf} \quad (23)$$

And:

$$(y_0 + \Delta y)^2 = 2de \sin \gamma - 2fd \cos \gamma + e^2 + f^2 + d^2 \quad (24)$$

$$\Delta y = \sqrt{2de \sin \gamma - 2fd \cos \gamma + d^2 + e^2 + f^2} - y_0$$

$$\sin \gamma = \frac{vt}{\sqrt{c^2 + (vt)^2}}, \cos \gamma = \frac{c}{\sqrt{c^2 + (vt)^2}} \quad (25)$$

$d$  In order to support the distance between the fulcrum of the cylinder and the pivot point of the telescopic boom;  $e$  the vertical distance between the pivot point of the telescopic boom and the pivot point of the supporting cylinder;  $\beta$  the auxiliary angle added to facilitate the geometric relationship;  $f$  The distance of the supporting device.

## 4 Analysis of joint simulation results

The control system uses the direct feedback control of the position of the optimized parameters. Based on the joint simulation technology, the combined motion control is realized. The results of the ADAMS post-processing unit are used to view the trajectory of the telescopic boom end and the simulation results of the dynamic characteristics. The results are analyzed.

### 4.1 Control parameter optimization

The control parameters are set using the Ziegler-Nichols tuning technique. he closed-loop control loop is established to determine the stability limit. The control parameters are calculated according to the formula shown in Equation (26)

$$k_p = 0.6K_{pc}, \quad k_i = \frac{k_p}{T_n}, \quad k_d = k_p T_v$$

$$T_n = 0.5T_c, \quad T_v = 0.12T_c \quad (26)$$

In the formula,  $K_{pc}$  the critical coefficient for the stability limit;  $T_c$  the critical oscillation period;  $T_n$  the integral time;  $T_v$  the derivative time;  $k_p, k_i, k_d$  corresponding to the three control parameters; Through the initial determination of the three parameters of the PID controller, and then fine-tuning to get better control of the control parameters. The tuning result is shown in Figure 6:

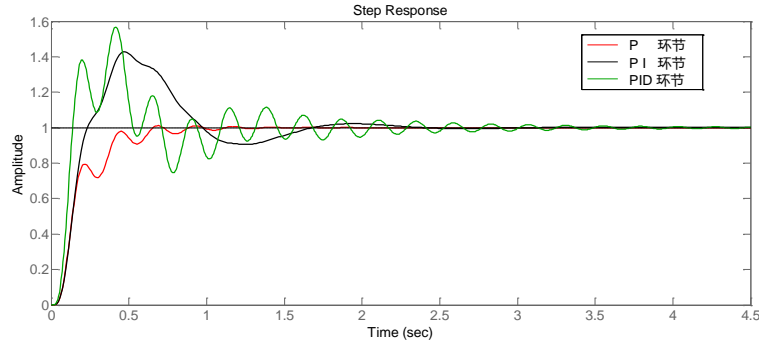


Fig.6 PID parameter setting result

As can be seen from the figure, the PID parameter is set:  $P=0.0621$ ,  $T_i=0.1973$ ,  $T_d=0$ . After adding the mechanical system, in order to improve the response speed of the system, it can adjust the value of  $T_d$  small range, because the integration time of the sensitivity of the disturbance, so for different environments, the value of the size of the need for further adjustment.

#### 4.2 simulation results

ADAMS results in the use of post-processing module, the end of the movement after the telescopic arm trajectory of the most front-end tracing out. Figure 7 (a) for the vertical plane of the trajectory of the movement of linear motion, the performance of the foremost telescopic arm along a vertical line; (c) shows the horizontal plane of the trajectory of the movement, (b) shows the trajectory of a linear motion in the spatial range, in which the foremost end of the telescopic arm moves along a straight line in the spatial range. The red line segment is the trajectory from the initial position to the ending position, which is obtained by the ADAMS track curve module.

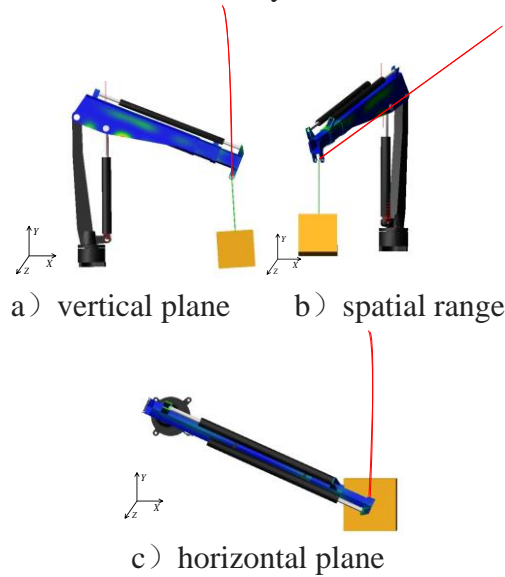


Fig.7 Results trajectory under three forms of exercise

#### 4.3 Combined motion characteristics analysis

According to the mark point selected by the foremost end of the telescopic arm, the movement of the telescopic boom is analyzed according to the expected trajectory by observing the position change of the marker in the space coordinate system. Figure 8 for the vertical plane linear motion simulation results:

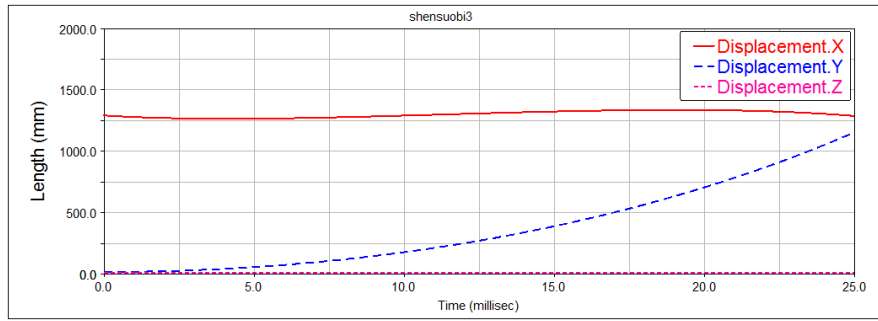


Fig.8 Vertical plane linear motion simulation results

It can be seen from the curve that the X-axis coordinate of the trajectory of the front end of the telescopic boom is linear, but fluctuates because the flexible arm flexes during the movement of the telescopic boom, Slider, resulting in telescopic arm movement during the deviation, through the feedback control adjustment, the final load transferred to the expected position. The Y-axis shows a gradual increase in pitch motion and the Z-axis does not change, indicating that no rotary motion is performed.

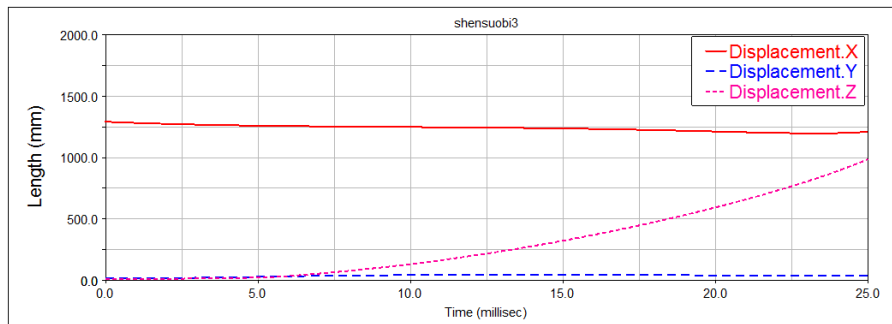


Fig.9 Horizontal plane linear motion simulation results

Figure 9 shows the horizontal plane motion simulation results, the curve shows that the trajectory of the front end of the telescopic arm X-axis coordinate of the whole trend is straight, but the curve slightly tilted, because the telescopic arm movement, the weight of flexible Arm flexure deformation, and telescopic arm section between the slider friction damping effect, resulting in telescopic arm movement during the expansion and contraction speed and the expected speed value of a certain deviation. The motion of the slewing mechanism is uniform motion according to the expectation, but in the running process of the slewing mechanism, due to the matching error of the rotating mechanism and the sway of the hoisting weight, the swivel speed is unstable. By feedback control of the control system, So that the deviation between the reproduced position and the expected position is reduced. The Z-axis gradually increases to indicate that the slewing angle is increased and the Y-axis remains unchanged to indicate that no pitching motion is performed.

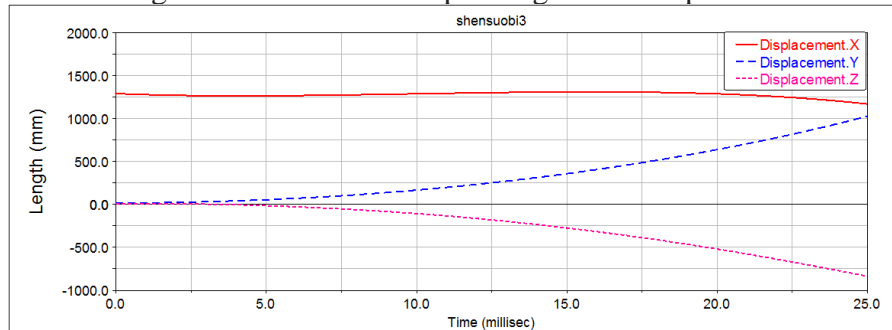


Fig.10 The spatial extent of linear motion simulation results

Figure 10 shows the simulation results for the spatial range linear motion. It can be seen from the curve that the overall X-axis coordinate of the trajectory of the linear motion of the front end of the telescopic arm is a straight line, but the expected positional deviation is larger than that of the combined movement of the two actions. This is because during the movement of the telescopic arm, the movement error comes from the friction factor of the telescopic process, bending deformation,

mechanical error of the rotation process, the weight of swing error. Y-axis and Z-axis are gradually changing, indicating that the telescopic boom in the lifting and rotating state, the feedback control of each institution, by constantly modifying the adjustment control parameters, making the position error decreases, but can not be completely eliminated.

## 5 Experiment

The experimental platform consists of mechanical system, hydraulic drive system, data acquisition system and measurement and control system. Figure 11 shows the experimental platform schematic. Figure 12 shows the experimental platform control system block diagram.

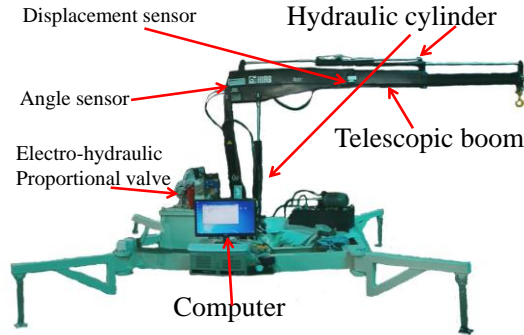


Fig.11 Experimental environment

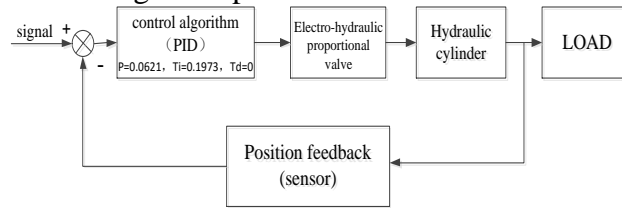


Fig.12 Control system block diagram

The simulation results of the vertical plane linear motion are selected, and the data of the arm length and pitch angle changes are compared with the experimental results, and the simulation results are compared with the experiment results under the no load and load conditions. Whether consistent. As shown in Fig.12 and Fig.13, the simulation results are compared with the experimental results.

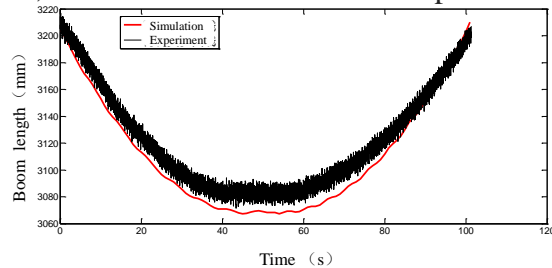


Fig.12 Simulation and Experimental results of Boom length

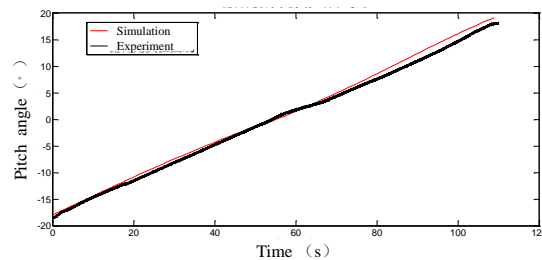


Fig.13 Simulation and Experimental results of Pitch angle

The simulation results of the multi-stage flexible telescopic boom simulation system and the experimental platform to compare the results obtained:



1) The simulation results are in good agreement with the experimental curves. The red line in the figure shows the result of the simulation, and the black line shows the result of the experiment. From the trend of the two curves can be seen that the simulation results more in line with the actual situation.

2) The main sources of error between the simulation results and the experimental results are: oil temperature of the hydraulic system, hydraulic valve dead zone, mechanical system gap, friction damping and other factors will make the movement lag, accompanied by a certain rock. These unmeasurable factors are difficult to add to the simulation model, so some errors will occur.

## 6 Conclusion

By describing three typical movements of the telescopic boom crane during the process of reloading, the motion process is simplified to a geometric model, and the law of input variation in accordance with the trajectory is obtained. Through the optimization of the control parameters, the combined motion control under three typical operating conditions is realized. ADAMS environment observed in the telescopic arm trajectory in line with the expected front-end linear motion requirements. At the same time, the experiment verifies the correctness of the model, and shows that the combined motion control of the model conforms to the request of telescopic arm.

The innovative point of this paper is to add a hydraulic control system to the combined motion of a given law based on the mechanical model of the telescopic boom with the multi-arm, fully flexible and inter-arm force restraints. The research contents can be used for reference in the process of crane's reloading, improving the efficiency of reprinting and reducing the number of physical prototype test.

## References

- [1] Zhang Yong-de, Wang Yang-tao, Wang Mo-nan, Jiang Jin-gang. Co-simulation of Flexible Body Based on ANSYS and ADAMS[J]. 2008, 20(17):4051-4052. (in Chinese)
- [2] LIU Pengfei. Research on Straight Trajectory Control of Telescopic Boom Aerial Work Platform[D]. Dalian: Dalian University of Technology, 2012
- [3] TENG Ruming. Rapid Design and Motion Planning of Boom System for the Aerial Work Platform[D]. Dalian: Dian University of Technology, 2012
- [4] LI Yuhong, NIE Lingxiao. ADAMS virtual prototype-based multi-body system dynamics simulation[J]. Engineering Journal of Wuhan University, 2010, 43(6): 758-760. (in Chinese)
- [5] DONG Fuxiang, HONG Jiazhen. Review of impact problem for dynamics of multibody system[J]. Advances in mechanics. 2009, 39(3): 352-354. (in Chinese)
- [6] SHEN Xiao-dong, LIU Chang-yi, ZHANG bo-shou. Dynamic simulation of Robotic Drilling Process with Joint Flexibility Considered[J]. Machinery Design & Manufacture. 2015, 3(3): 196-197. (in Chinese)
- [7] ZHONG Xiang-qiang. LIANG Li-dong. Coupling Simulation for Hydraulic Excavator's Working Mechanism[J], Machinery Design & Manufacture. 2012, 6(6): 229—230. (in Chinese)
- [8] LI Yuhong, NIE Lingxiao. ADAMS virtual prototype-based multi-body system dynamics simulation[J]. Engineering Journal of Wuhan University, 2010, 43(6): 758-760. (in Chinese)
- [9] Wang Dan, Liu Hongyi, Liu Mingchen, Zhang Shengnan. The Virtual Prototype Model and Dynamics Simulation for the Laying Pipe Manipulator By Using Adams Software[J]. Mechanical Science and Technology for Aerospace Engineering. 2013, 32(11), 1644-1646. (in Chinese)
- [10] Yu Hanxiang, Yu Lanfeng, Li Shaopeng. Finite Element Analysis of the Contact Problem on the Telescopic Boom of Hydraulic Aerial Cage[J]. Mechanical Science and Technology for Aerospace Engineering. 2014, 33(12), 1773-1775. (in Chinese)